Insect Molecular Biology

Insect Molecular Biology (2016) **25**(5), 550–565 doi: 10.1111/imb.12242

RNA interference-mediated knockdown of the Halloween gene *Spookiest* (CYP307B1) impedes adult eclosion in the western tarnished plant bug, *Lygus hesperus*

E. Van Ekert*, M. Wang†, Y.-G. Miao†, C. S. Brent* and J. J. Hull*

**USDA-ARS Arid Land Agricultural Research Center, Maricopa, AZ, USA; and* †*Zhejiang University, Hangzhou, China*

Abstract

Ecdysteroids play a critical role in coordinating insect growth, development and reproduction. A suite of cytochrome P450 monooxygenases coded by what are collectively termed Halloween genes mediate ecdysteroid biosynthesis. In this study, we describe cloning and RNA interference (RNAi)-mediated knockdown of the CYP307B1 Halloween gene (*Spookiest*) in the western tarnished plant bug, *Lygus hesperus*. Transcripts for *Ly. hesperus Spookiest* (*LhSpot*) were amplified from all life stages and correlated well with timing of the pre-moult ecdysteroid pulse. In adults, *LhSpot* was amplified from heads of both genders as well as female reproductive tissues. Heterologous expression of a LhSpot fluorescent chimera in cultured insect cells co-localized with a fluorescent marker of the endoplasmic reticulum/secretory pathway. RNAi-mediated knockdown of *LhSpot* in fifth instars reduced expression of ecdysone-responsive genes *E74* and *E75*, and prevented adult development. This developmental defect was rescued following application of exogenous 20-hydroxyecdysone but not exogenous 7-dehydrocholesterol. The unequivocal RNAi effects on *Ly. hesperus* development and the phenotypic rescue by 20-hydroxyecdysone are causal proof of the involvement of LhSpot in ecdysteroid biosynthesis and related developmental processes, and may provide an avenue for development of new control measures against *Ly. hesperus*.

Keywords: western tarnished plant bug, *Lygus hesperus*, Halloween gene, *Spookiest*, CYP307B1, RNA interference.

First published online 18 May 2016.

Correspondence: J. Joe Hull, USDA-ARS Arid Land Agricultural Research Center, 21881 N Cardon Lane, Maricopa, AZ 85138, USA. Tel.: + 1 520 316 6334; fax: + 1 520 316 6330; e-mail: joe.hull@ars.usda.gov

E. Van Ekert and M. Wang contributed equally to this work.

Introduction

In insects, the fundamental processes of growth, development and reproduction are coordinated by fluctuations in the level of circulating ecdysteroids, the major forms of which include ecdysone (E) and its derivative 20-hydroxyecdysone (20E). During pre-adult development, pulses of 20E trigger moulting and metamorphosis, whereas in adult females, 20E functions in oogenesis, vitellogenesis, choriogenesis and the early events of embryogenesis (Morgan & Poole, 1977; Koolman, 1982; Gilbert *et al*., 2002; Truman, 2005). Similar to vertebrate steroidal biosynthesis pathways, insects utilize cholesterol and/or plant sterols as ecdysteroid precursors (Gilbert *et al*., 2002; Niwa & Niwa, 2011); however, unlike vertebrates, insects lack genes such as squalene synthase that are critical for synthesizing cholesterol from simple precursor molecules (Gilbert *et al*., 2002; Niwa & Niwa, 2011). Consequently, ecdysteroid biosynthesis must rely on dietary supplied cholesterol (obtained directly from prey by carnivorous insects) or plant-derived phytosterols, which must first undergo dealkylation to cholesterol in midgut cells (Gilbert *et al*., 2002; Gilbert & Warren, 2005; Canavoso *et al*., 2001). The absorbed cholesterol is transported via haemolymph lipophorin to steroidogenic organs (prothoracic glands in immatures and ovarian follicle cells in adult females) where it is step-wise converted to E by a series of conserved enzymatic reactions (Fig. 1). The best-characterized genes in this pathway are the Halloween genes, a suite of cytochrome P450 monooxygenases

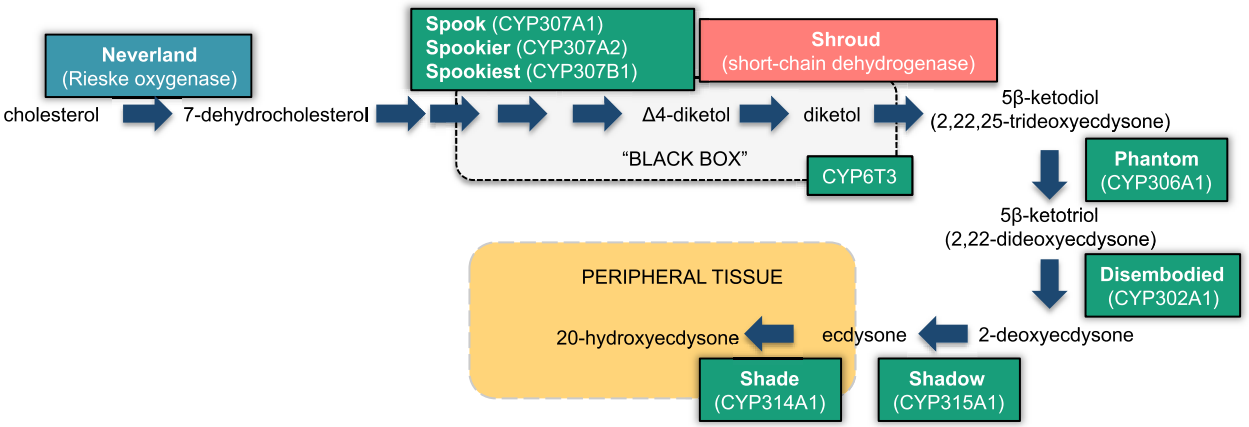

Figure 1. Current model of the ecdysteroid biosynthetic pathway in insects.

initially identified in *Drosophila melanogaster* developmental mutants (Jürgens *et al.*, 1984; Nüsslein-Volhard *et al.*, 1984; Wieschaus *et al.*, 1984).

The initial step in the ecdysteroid biosynthetic pathway, conversion of cholesterol to 7-dehydrocholesterol, is mediated by a Rieske-domain oxygenase termed Neverland that catalyses 7,8,-dehydrogenation of the cholesterol precursor. The steps converting the 7-dehydrocholesterol into 5β-ketodiol (2,22,25-trideoxyecdysone) involve multiple enzymatic steps currently known to be mediated by a short-chain dehydrogenase termed Shroud, a P450 monooxygenase(s) CYP307A1/A2 termed Spook/Spookier, and a CYP6T3 monooxygenase (Iga & Kataoka, 2012; Niwa & Niwa, 2014). Although Δ4-ketodiol and diketol have been identified as likely intermediate substrates, additional substrates and the precise nature of the reactions that yield 5β-ketodiol have yet to be fully elucidated. Consequently, these steps are frequently referred to as the 'black box' of ecdysteroid biosynthesis (Namiki *et al.*, 2005; Ono *et al.*, 2006; Rewitz *et al.*, 2007). 5β-ketodiol is further hydroxylated to yield 5β-ketotriol (2,22-dideoxyecdysone), 2-deoxyecdysone and E by the Phantom, Disembodied and Shadow P450 monoxygenases, respectively. E is then converted in peripheral tissues into the active hormone, 20E, by the P450 monoxygenase Shade.

Given the indispensable role of ecdysteroids in regulating and coordinating the critical insect processes of growth, development and reproduction, the lack of functional redundancy amongst the Halloween suite of genes is surprising. Identification or prediction of Halloween genes in diverse insect species (Namiki *et al.*, 2005; Ono *et al.*, 2006, 2012; Sztal *et al.*, 2007; Christiaens *et al.*, 2010; Iga & Smagghe 2010; Marchal *et al.*, 2010; Yamazaki *et al.*, 2011; Hentze *et al.*, 2013; Jia *et al.*, 2013a,b; Luan *et al.*, 2013; Pondeville *et al.*, 2013; Zhou *et al.*, 2013; Shahzad *et al.*, 2015), as well as other arthropods (Rewitz & Gilbert, 2008; Cabrera *et al.*, 2015), has revealed that each gene is more similar to its respective orthologues than to other P450 monoxygenases, suggesting the specific steps in ecdysteroid biosynthesis are catalysed by a single enzyme. Paralogues, however, have been identified for the CYP307 P450 monoxygenases, which have undergone lineage-specific duplications/losses, with three paralogues CYP307A1 (Spook, Spo), CYP307A2 (Spookier, Spok) and CYP307B1 (Spookiest, Spot) identified in various species, albeit with only two of the three present in any one species (Rewitz *et al.*, 2007; Sztal *et al.*, 2007; Rewitz & Gilbert, 2008). In *Dr. melanogaster*, duplication of the ancestral *Spok* gene, thought to be specific to the Drosophilidae, probably yielded *Spo*. *Spok*-like sequences, however, have recently been annotated in *Chilo suppressalis* (AHW57298) (Wang *et al.*, 2014), *Cnaphalocrocis medinalis* (AJN91167), *Dendroctonus armandi* (ALD15893) (Dai *et al.*, 2015), *Nilaparvata lugens* (AIW79977) and *Laodelphax striatellus* (AGU16448) (Jia *et al.*, 2015), with RNA interference (RNAi)-based knockdown in the last species reportedly supporting a functional role in development. The third paralogue, *Spot*, is thought to be a lineage-specific duplication of *Spo*. To date, *Spot*-like sequences have been identified/predicted in *Aedes aegypti* (Rewitz *et al.*, 2007), *Anopheles gambiae* (Rewitz *et al.*, 2007) and *Tribolium castaneum* (Rewitz *et al.*, 2007; Christiaens *et al.*, 2010). In *Apis mellifera*, *Spot* appears to be the only CYP307 paralogue (Rewitz *et al.*, 2007; Yamazaki *et al.*, 2011). This paralogue reduction is not characteristic of the Hymenoptera, as the lone CYP307-like sequence in *Nasonia vitripennis* shares greater homology with Spo than Spot (Rewitz *et al.*, 2007). Initial analysis of the *Acyrthosiphon pisum* genome suggested the presence of three *Spo*-like sequences (Ap-Spo1–3; XM_001945726, XM_001946260 and XM_001948680)

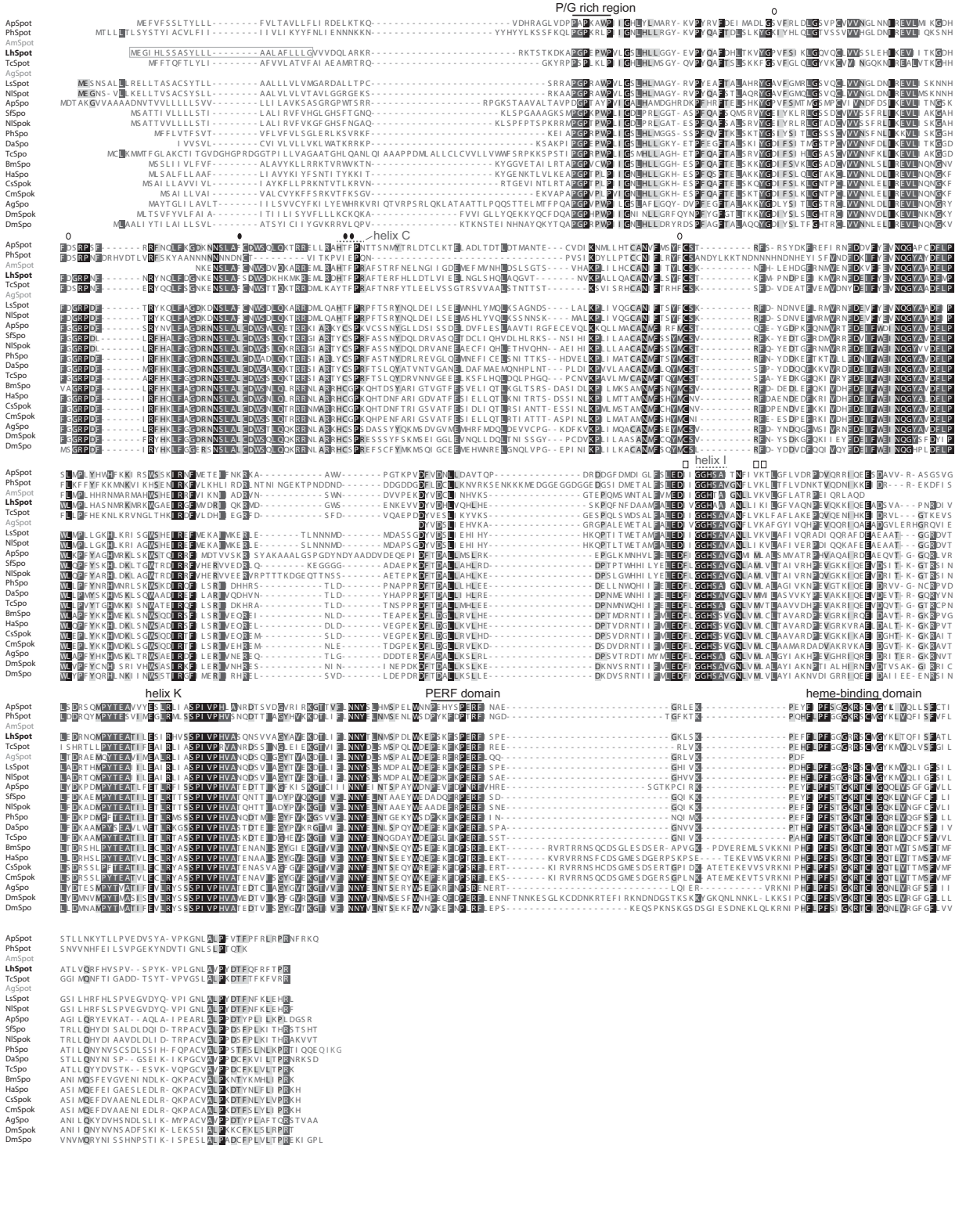

with the first two genes proposed as *Spo* orthologues and the third as a *Spot* orthologue (Christiaens *et al.*, 2010). Subsequent genome annotations have collapsed the *Spo* paralogues into a single gene.

Whereas the molecular basis of ecdysteroid biosynthesis has been extensively characterized in holometabolous insects, our understanding of this pathway in hemimetabolous insects is limited to a few species –

Figure 2. Multiple sequence alignment of *Lygus hesperus* Spookiest (LhSpot) with Spook paralogues from 14 insect species. Sequences were aligned using MUSCLE (Edgar, 2004) with default settings. Amino acids highlighted in black indicate amino acid identity whereas those in grey represent amino acid conservation. Characteristic P450 domains/motifs (Pro/Gly rich region, helix K, Pro-Glu-Arg-Phe (PERF) domain and heme-binding domain) are indicated. The helix C and helix I motifs (dashed lines with grey font) do not meet conventional definitions for these regions (ie helix C = WXXXR; helix I = GxE/DTT/S) but correspond to regions defined as such in reports of insect CYP307A1 orthologues (Iga & Smagghe, 2010; Jia *et al.*, 2015; Shahzad *et al.*, 2015). Amino acid substitutions specific to Spot paralogues that are located near the putative helix C are indicated with closed ovals, those near helix I with open squares and miscellaneous spot specific changes are indicated with open ovals. Residues comprising the *Ly. hesperus* Spot hydrophobic targeting sequence are outlined. Abbreviations: ApSpot, *Acyrthosiphon pisum* Spookiest (XP_001948715); PhSpot, *Pediculus humanis corporis* Spookiest (XP_002425350); AmSpot, *Apis mellifera* Spookiest (BAJ54121); LhSpot, *Ly. hesperus* Spookiest; TcSpot, *Tribolium castaneum* Spookiest (EFA05673); AgSpot, *Anopheles gambiae* Spookiest (AAV28189); LsSpot; *Laodelphax striatellus* Spookiest (AGI92303); NlSpot, *Nilaparvata lugens* Spookiest (AIW79978); ApSpo, *Ac. pisum* Spook (XP_001945761); SfSpo, *Sogatella furcifera* Spook (AGU16443); NlSpok, *Ni. lugens* Spookier (AIW79977); PhSpo, *Pe. humanis corporis* Spook (XP_002429996); DaSpo, *Dendroctonus armandi* Spook (ALD15893); TcSpo, *T. castaneum* Spook (EFA11558); BmSpo, *Bombyx mori* Spook (BAM73857); HaSpo, *Helicoverpa armigera* Spook (AID54856); CsSpok, *Chilo suppressalis* Spookier (AHW57298); CmSpok, *Cnaphalocrocis medinalis* Spookier (AJN91167); AgSpo, *An. gambiae* Spook (AHB59617); DmSpok, *Drosophila melanogaster* Spookier (EDP28053); DmSpo, *Dr. melanogaster* Spook (AAQ05973).

Ac. pisum (Christiaens *et al.*, 2010), *Bemisia tabaci* (Luan *et al.*, 2013), *La. striatellus* (Jia *et al.*, 2013a, 2014, 2015; Wan *et al.*, 2014a,b) and *Sogatella furcifera* (Jia *et al.*, 2013b; Wan *et al.*, 2014c). Excluded from this list are mirid plant bugs, many of which are polyphagous agricultural pests (Wheeler, 2001; Schuh, 2013). One genus of this group that is of particular economic importance is *Lygus*. Traditionally managed with broad-spectrum insecticides, reports of insecticide resistance in field populations (Snodgrass, 1996; Snodgrass & Scott, 2002; Snodgrass *et al.*, 2009) underscore the need for alternative control tactics. One promising area for potential development is targeting the molecular machinery that regulates developmental and reproductive processes, such as those controlled by ecdysteroids. A generally poor understanding of the underlying physiology and limited molecular resources have hampered efforts to devise such approaches for *Lygus*. Recent transcriptome assemblies (Hull *et al.*, 2013, 2014) for the western tarnished plant bug (*Lygus hesperus* Knight), the dominant pest *Lygus* species in the western USA (Schwartz & Footit, 1998), have however greatly facilitated gene identification and annotation processes and have opened the possibility of exploring gene functionality through the use of RNAi-mediated knockdown. Furthermore, we recently demonstrated the criticality of ecdysteroid timing in controlling the nymphal–adult moult in *Ly. hesperus* (Brent *et al.*, 2016). In this study, we build on those findings and report transcriptome-based identification of a single *Spo*-like sequence that shares significantly greater sequence homology with Spot orthologues than with either Spo or Spok. The transcript is expressed in select adult tissues and throughout development, with transcript abundance fluctuating inversely with previously reported ecdysteroid levels. RNAi-mediated knockdown and subsequent 20E rescue confirm the importance of the *LhSpot* transcript in controlling the timing of adult eclosion and development of adult characteristics. These are important initial steps toward developing control approaches that target a potential vulnerability of this key pest.

Results

Identification and phylogenetic characterization of LhSpot

To identify the first cytochrome P450-catalysed step in *Ly. hesperus* ecdysteroid biosynthesis (ie CYP307), we performed a tBLASTn search of our recent transcriptome assembly (Hull *et al.*, 2014) using queries consisting of representative Spo sequences from five insect orders: Diptera (*Dr. melanogaster*), Lepidoptera (*Bombyx mori*), Hymenoptera (*Na. vitripennis*), Coleoptera (*T. castaneum*) and Hemiptera (*Ac. pisum* and *La. striatellus*). All of the queries generated the same unigene hit with an *e*-value $< 10^{-127}$. The next closest unigene hits had *e*-values ranging between 10^{-32} to 10^{-46}, none of which exhibited homology with the Halloween genes, suggesting the presence of a single *Spo*-like sequence in our transcriptome assembly. Multiple Spo paralogues (ie Spo, Spok and Spot), however, have been reported in various species from multiple insect orders (Rewitz *et al.*, 2007). The presence of a single sequence in *Ly. hesperus* may be the result of exclusion of temporally or spatially restricted transcripts (eg transcripts specifically regulated in development) in our transcriptome assembly, or alternatively may reflect loss of those genes.

Using cDNA generated from fifth instars 2 days after the moult and primers designed to the putative *Spo*-like open reading frame (ORF), we amplified a 1482-nucleotide (nt) product that encodes a 493-amino acid protein with a predicted molecular weight of 56.1 kDa. The unigene ORF shares considerable identity (54.7%) with a putative Spo orthologue in the hemipteran pest, *La. striatellus* (AGI92303), but only moderate identity (~37%) with Spo orthologues in *Dr. melanogaster* (AAQ05973), *Bo. mori* (BAM73857) and *Ac. pisum* (XP_001945761). Despite relatively low sequence identity, the *Ly. hesperus* sequence contains motifs characteristic of insect cytochrome P450s (Werck-Reichhart & Feyereisen, 2000) including a heme-binding loop (PFxxGxRxCxG), helix K (ExxR) and an aromatic PERF

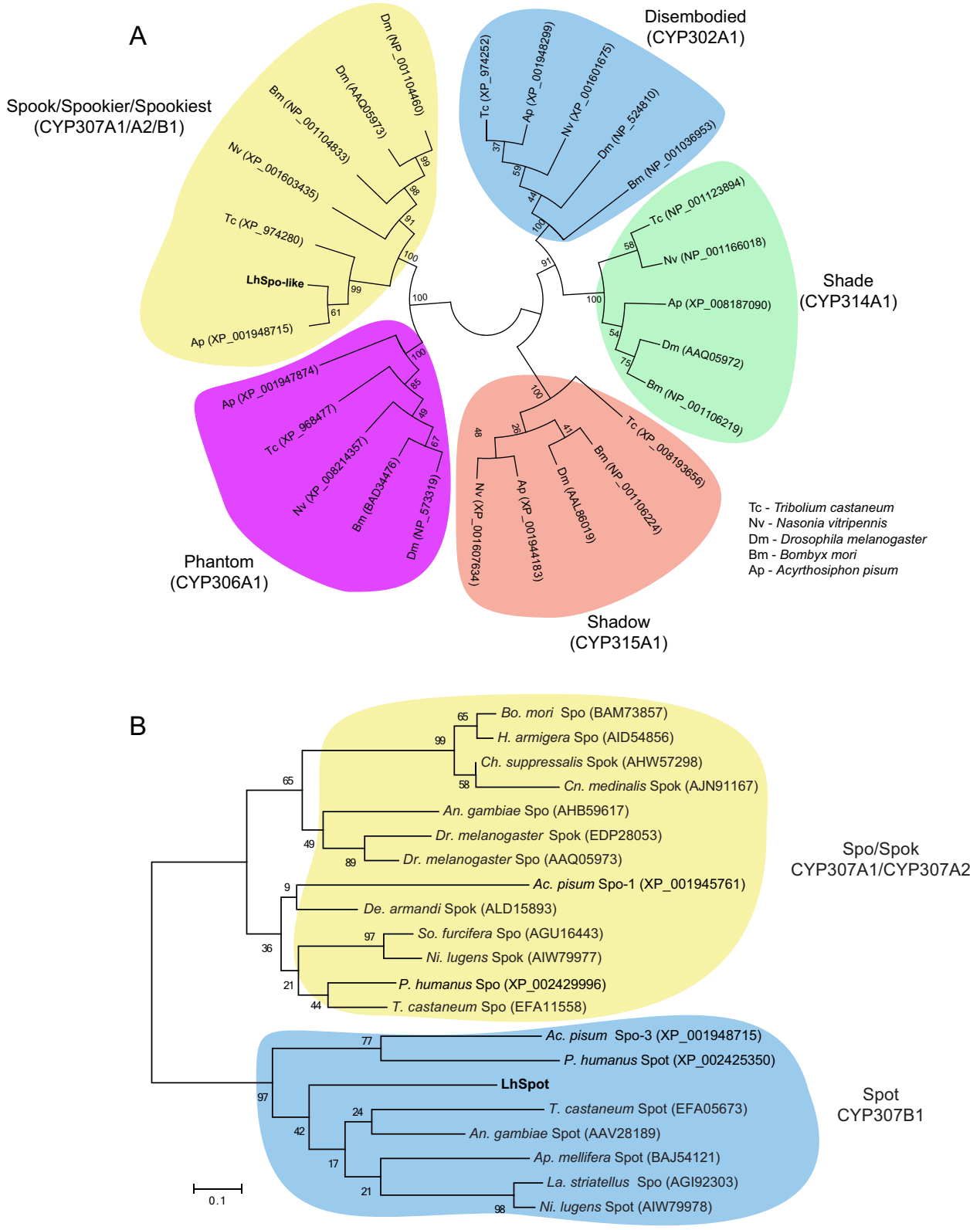

domain (PxxFxPE/DRF) (Fig. 2). Although the consensus sequences for two additional P450 motifs, helix C (WxxxR) and helix I (A/GGxD/ETT/S), have diverged from that seen in the other Halloween proteins (Namiki *et al.*, 2005; Ono *et al.*, 2006; Iga & Smagghe, 2010; Marchal *et al.*, 2011; Zhou *et al.*, 2013; Cabrera *et al.*,

Figure 3. Phylogenetic relationships of the putative *Lygus hesperus* Spookiest (LhSpot) sequence. (A) Phylogenetic analysis using full-length Halloween protein sequences from five insect species. The respective sequences were aligned using MUSCLE (Edgar, 2004) and the evolutionary history was inferred using the maximum likelihood method implemented in MEGA6 (Tamura *et al.*, 2013). The bootstrap consensus tree is based on 1000 replicates with support values indicated at the branch points. Accession numbers of the sequences used in the analysis are indicated in parentheses and can be found in Table S3. (B) Phylogenetic relationships amongst the CYP307 group of Halloween genes. The analysis was performed as above using the CYP307A1-like sequences from Fig. 2. The evolutionary history was inferred using the maximum likelihood method based on the Jones Thornton-Taylor (JTT) matrix-based model. The tree with the highest log likelihood (−1496.1948) is shown. The percentage of trees in which the associated taxa clustered together is shown next to the branches. The tree is drawn to scale, with branch lengths measured in the number of substitutions per site. Sequence accession numbers are indicated in parentheses. Species abbreviations are: *Ac. pisum, Acyrthosiphon pisum*; *An. gambiae*, *Anopheles gambiae*; *Ap. mellifera*, *Apis mellifera*; *Bo. mori*, *Bombyx mori*; *Ch. suppressalis*, *Chilo suppressalis*; *Ch. medinalis*, *Cnaphalocrocis medinalis*; *De. armandi, Dendroctonus armandi*; *Dr. melanogaster*, *Drosophila melanogaster*; *H. armigera*, *Helicoverpa armigera*; *La. striatellus*, *Laodelphax striatellus*; *Ni. lugens*, *Nilaparvata lugens*; *P. humanus*, *Pediculus humanus corporis*; *So. furcifera*, *Sogatella furcifera*; *T. castaneum*, *Tribolium castaneum*.

2015; Jia *et al.*, 2015; Shahzad *et al.*, 2015), the regions associated with these motifs are well conserved in the LhSpo-like sequence and orthologues in other species (Fig. 2).

To further confirm annotation of the unigene sequence, we examined its phylogenetic relationship with Halloween proteins in *Dr. melanogaster*, *Bo. mori*, *Na. vitripennis*, *Ac. pisum* and *T. castaneum* (Fig. 3A). Consistent with the sequence analyses and the initial annotation, the unigene sequence aligned to the Spo clade, with highest similarity (as expected given the shared hemimetabolous lineage) to *Ac. pisum* Spo. To increase the phylogenetic resolution, we limited the analysis to 20 sequences annotated as Spo, Spok or Spot. When aligned with this larger clan-specific data set, sequence conservation between the unigene and the Spo/Spok orthologues averaged 38.5%, whereas in the Spot group identity was 48.6% (Table S1), suggesting that the LhSpo-like sequence is a Spot orthologue. Phylogenetic analyses (maximum likelihood, neighbour joining, minimum evolution and the Unweighted Pair Group Method with Arithmetic Mean method (UPGMA)) further support this designation as the LhSpo-like sequence clustered away from Spo and Spok in a largely Spot-specific clade (Fig. 3B). The lone exception to that clade is a sequence from *La. striatellus* (AGI92303) annotated as CYP307A1; however, given the phylogenetic relatedness with Spot we suggest that it has been misannotated in the database and that the *La. striatellus* sequence is actually a Spot orthologue. Based on these phylogenetic relationships and shared sequence similarities, we have annotated the *LhSpo*-like sequence as a *Spot* orthologue (LhSpot; GenBank accession KT818622).

Heterologous expression of a LhSpot fluorescent chimera in cultured insect cells

Spo homologues in *Dr. melanogaster* and *Bo. mori* co-localize in Drosophila S2 cells with markers of the endoplasmic reticulum (ER)/secretory pathway (Namiki *et al.*, 2005; Ono *et al.*, 2006). Cursory domain analyses (hydrophobic amino terminus with Pro/Gly-rich region), homology with microsomal cytochrome P450s and subcellular localization prediction algorithms (WoLF PSORT and Target P1.1) suggest that LhSpot also localizes to the ER/secretory pathway. To provide further insights into the presumptive subcellular localization of LhSpot, we co-expressed fluorescent chimeras of LhSpot (LhSpot-Venus) and the human KDEL (Lys-Asp-Glu-Leu) endoplasmic reticulum protein retention receptor (HsKDELR-mCherry), a marker of the ER/secretory pathway (van der Vlies *et al.*, 2002; Maroniche *et al.*, 2011), in cultured *Trichoplusia ni* cells. Cells expressing LhSpot-Venus exhibited a diffuse green fluorescent pattern typical of ER that extensively overlaid with the HsKDELR-mCherry red fluorescent signal (Fig. 4), suggesting co-localization of the two proteins. Although this cellular localization is consistent with previous studies and suggests that LhSpot resides

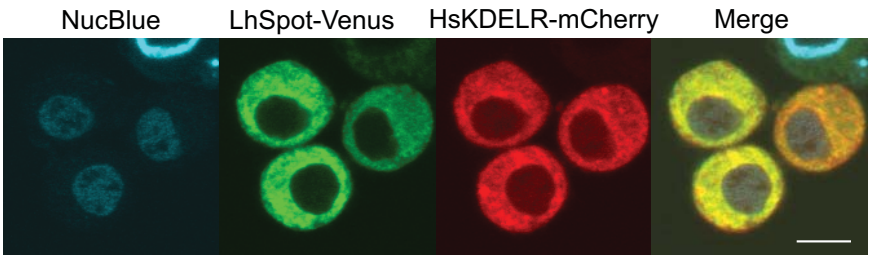

Figure 4. Subcellular localization of a fluorescent *Lygus hesperus* Spookiest (LhSpot) chimera in cultured insect cells. Cells were co-transfected with expression plasmids encoding LhSpot-Venus (green) and an endoplasmic reticulum marker (ER), *Homo sapiens* KDEL (Lys-Asp-Glu-Leu) endoplasmic reticulum protein retention receptor-mCherry (KDELR-mCherry; red). At 48 h post-transfection, cells were labelled with the nuclear marker NucBlue (blue) and live cells were imaged on a confocal scanning laser microscope using a 60× water objective. Overlay of the green and red fluorescent signals (yellow in the merge panel) suggests co-localization of LhSpot-Venus with KDELR-mCherry in the ER. Scale bar = 10 μm.

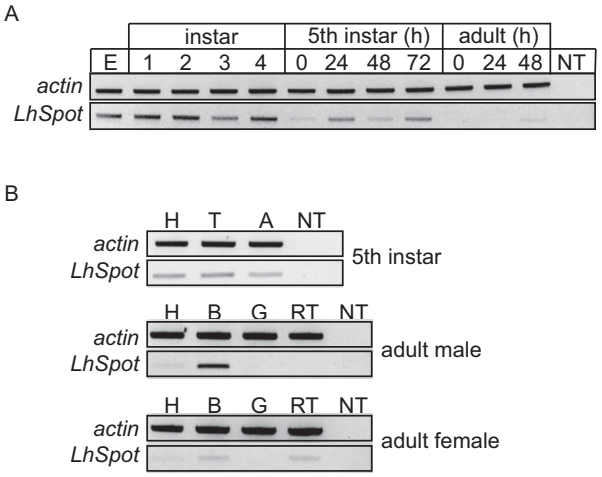

Figure 5. Reverse Transcription-PCR (RT-PCR) analysis of *Lygus hesperus Spookiest (LhSpot)* expression. (A) Developmental expression profile. *LhSpot* and *actin* (control gene) transcripts were amplified from eggs (E), first to fourth instars (1–4), fifth instars at four time intervals postmoult and adults at three intervals postmoult. (B) Tissue expression profile in fifth instars and adults of each gender. *LhSpot* and *actin* transcripts were amplified from head (H), thorax (T) and abdomen (A) in fifth instars, and head, body (B), midgut/hindgut (G) and reproductive tissue (RT) in mature adults. Female reproductive tissues include ovary and seminal depository; male reproductive tissues include testes and lateral/medial accessory glands. Amplimers correspond to ~500-bp fragments of the transcripts of interest. PCR products were electrophoresed in 1.5% agarose gels and stained with SYBR Safe. For better clarity, negative images of representative gel images are shown. NT, no template. Image shown is representative of three biological replicates.

in the ER/secretory pathway, *in vivo* confirmation of this finding in native tissues remains to be demonstrated.

Reverse Transcription-PCR (RT-PCR) expression profile of LhSpot

Spo orthologues have been reported to be expressed throughout embryonic and larval development as well as in select adult tissues (Rewitz *et al.*, 2007). We used RT-PCR to examine the temporal and spatial abundance of *LhSpot* transcripts. *LhSpot* transcripts were amplified from eggs and throughout nymphal development (Fig. 5A). To determine the potential role of *LhSpot* abundance in relation to the nymphal–adult moult, we examined expression at 24-h intervals from the initiation of the fifth instar until 48 h post-adult eclosion. *LhSpot* transcripts exhibited rhythmic expression, with levels peaking at 1 and 3 days after moulting to the fifth instar. Transcripts were barely detectable on the day of eclosion to the fifth instar and were completely undetectable in adults until 48 h post-eclosion (Fig. 5A). *LhSpot* was amplified from all three nymphal segments, but was spatially restricted in adults (Fig. 5B). In males, transcripts were amplified from bodies and to a lesser extent heads with no detectable amplification from male reproductive tissues (testes and accessory glands). In females, amplimers were detectable from head, bodies and reproductive tissue (ovary and seminal depository), albeit at varying abundances (Fig. 5B).

RNAi-mediated knockdown of LhSpot

To examine the functional role of LhSpot, we injected double-stranded RNAs (dsRNAs) corresponding to either a 547-bp fragment (nt 846–1352) of *LhSpot* or to the complete *enhanced green fluorescent protein* (*EGFP*) ORF into newly eclosed fifth instars. RT-PCR analysis of transcript levels at 48 h post-injection revealed reduced expression of *LhSpot* in the *LhSpot* dsRNA-injected nymphs compared with the non-injected and *EGFP* dsRNA-injected controls with no discernible effects on expression of the control genes *actin* and *glyceraldehyde 3-phosphate dehydrogenase* (*GAPDH*) (Fig. 6A). Because a reduction in *LhSpot* expression is expected to negatively affect ecdysteroid biosynthesis and thus ecdysone titres, we examined the effects of *LhSpot* knockdown on the expression of *E74* and *E75*, two ecdysone-inducible transcription factors (Thummel, 1996), as a proxy for measuring circulating ecdysone. Transcript levels of *E74* and *E75* were both reduced in nymphs injected with *LhSpot* dsRNA compared with controls (Fig. 6A), strongly suggesting that *LhSpot* knockdown had impacted ecdysteroid levels. We next examined the effects of *LhSpot* knockdown on adult development. At 3 days post-injection, we detected no noticeable phenotypic difference between *LhSpot* dsRNA-injected and control nymphs (Fig. 6B). However, consistent with a disrupted ecdysteroid signalling pathway, *LhSpot* dsRNA-injected nymphs failed to undergo adult eclosion and maintained a nymphal appearance (absence of wings and smaller size), albeit with elongated abdomens and black cuticular banding on the dorsum, even at >20 days post-injection (Fig. 6B). Surprisingly, despite the nymphal appearance, *LhSpot* dsRNA-injected nymphs at 25 days post-injection exhibited limited oogenesis producing a few stage 3 oocytes (Spurgeon & Brent, 2010) that are typically observed in young adult females (Fig. 6C).

More comprehensive analysis of the effects of *LhSpot* knockdown on the timing of adult development showed that eclosion typically occurred 3–4 days after treatment in non-injected, buffer-injected and *EGFP* dsRNA-injected nymphs, but was never achieved within the time frame (25 days post-injection) of our study (Fig. 7). Furthermore, nymphs injected with *LhSpot* dsRNA exhibited higher levels of mortality relative to controls that had undergone adult eclosion (Fig. 8), but persisted for longer than expected.

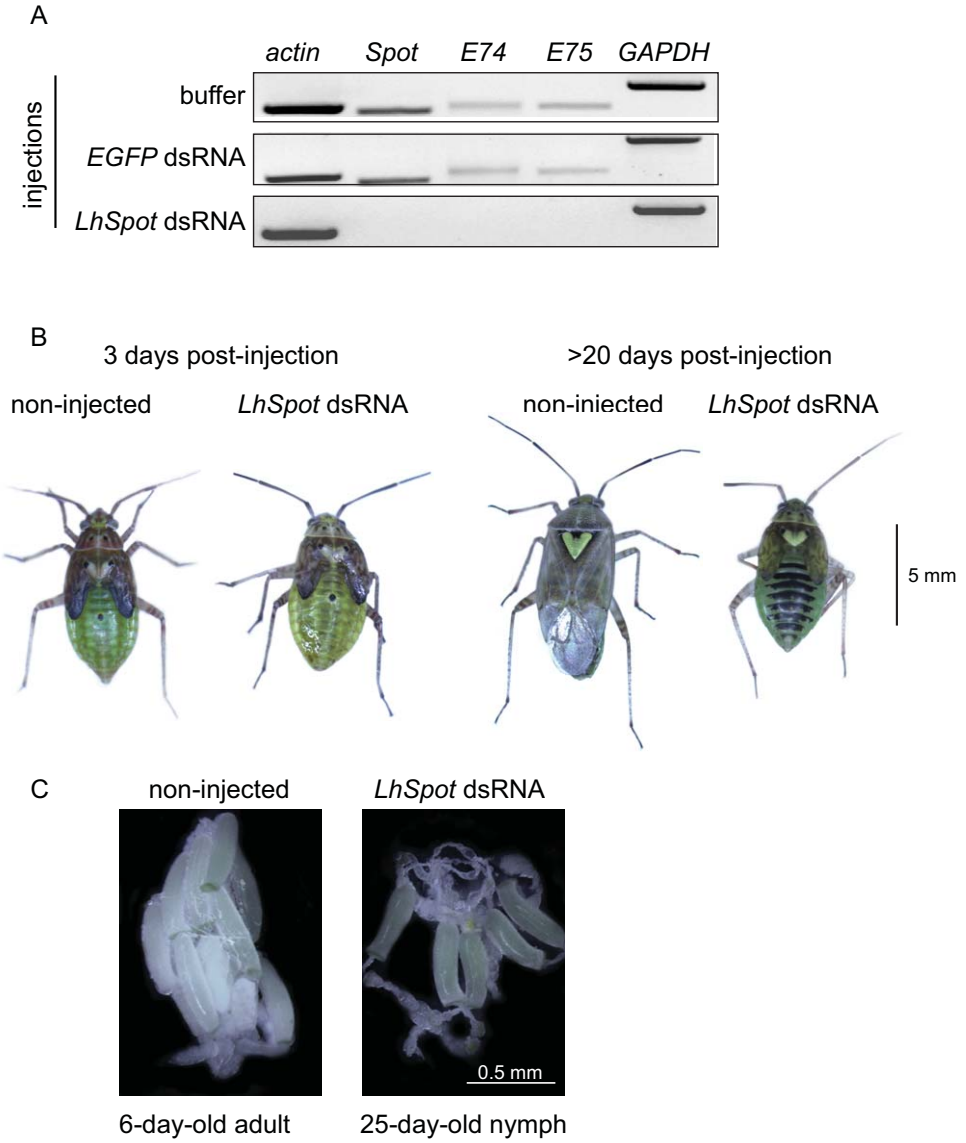

Figure 6. RNA interference-mediated knockdown of *Lygus hesperus Spookiest (LhSpot).* (A) *LhSpot* transcript expression is reduced following *LhSpot* double-stranded RNA (dsRNA) injection. Reverse Transcription-PCR (RT-PCR) amplification of the control genes *actin* and *glyceraldehyde 3-phosphate dehydrogenase* (GAPDH) along with two ecdysone responsive genes (*E74* and *E75*) and *LhSpot* in non-injected, *enhanced green fluorescent protein* (*EGFP*) dsRNA-injected and *LhSpot* dsRNA-injected nymphs at 48 h post-injection. Amplimers correspond to ~500-bp fragments of the transcripts of interest except for *GAPDH*, which was full length. PCR products were electrophoresed in 1% agarose gels and stained with SYBR Safe. For better clarity, negative images of representative gel images are shown. Image shown is representative of three biological replicates. (B) *LhSpot* knockdown prevents adult eclosion. Non-injected newly emerged fifth instars and nymphs injected with *LhSpot* dsRNA were imaged 3 days post-injection and > 20 days post-injection. Non-injected controls underwent adult eclosion, whereas *LhSpot* dsRNA-injected nymphs retained a nymphal phenotype but continued to grow and developed abdominal pigmentation. (C) Oogenesis in *LhSpot* dsRNA-injected nymphs. Representative images of ovaries from a 6-day-old untreated adult female and a nymph > 20 days after injection with *LhSpot* dsRNA.

Effects of exogenous 20E and 7-dehydrocholesterol following LhSpot *knockdown*

As Spot catalyses a relatively early step in 20E biosynthesis (presumably within the so-called 'black box'), we hypothesized that application of ecdysteroids (eg 20E) upstream of that step should be able to rescue the knockdown phenotype as demonstrated in other systems (Ono *et al.*, 2006; Jia *et al.*, 2015; Shahzad *et al.*, 2015). Topical application of 20E 24 h post-*LhSpot* dsRNA injection rescued adult eclosion (Fig. 9A). Non-treated and ethanol (20E vehicle) treated nymphs failed to enter the final moult. The rescue effect appeared to be highly time-dependent, as addition of 20E at the time of injection or later than 24 h post-injection either failed to rescue adult eclosion or resulted in partial eclosion with the adults trapped in the old exoskeleton (Fig. 9B).

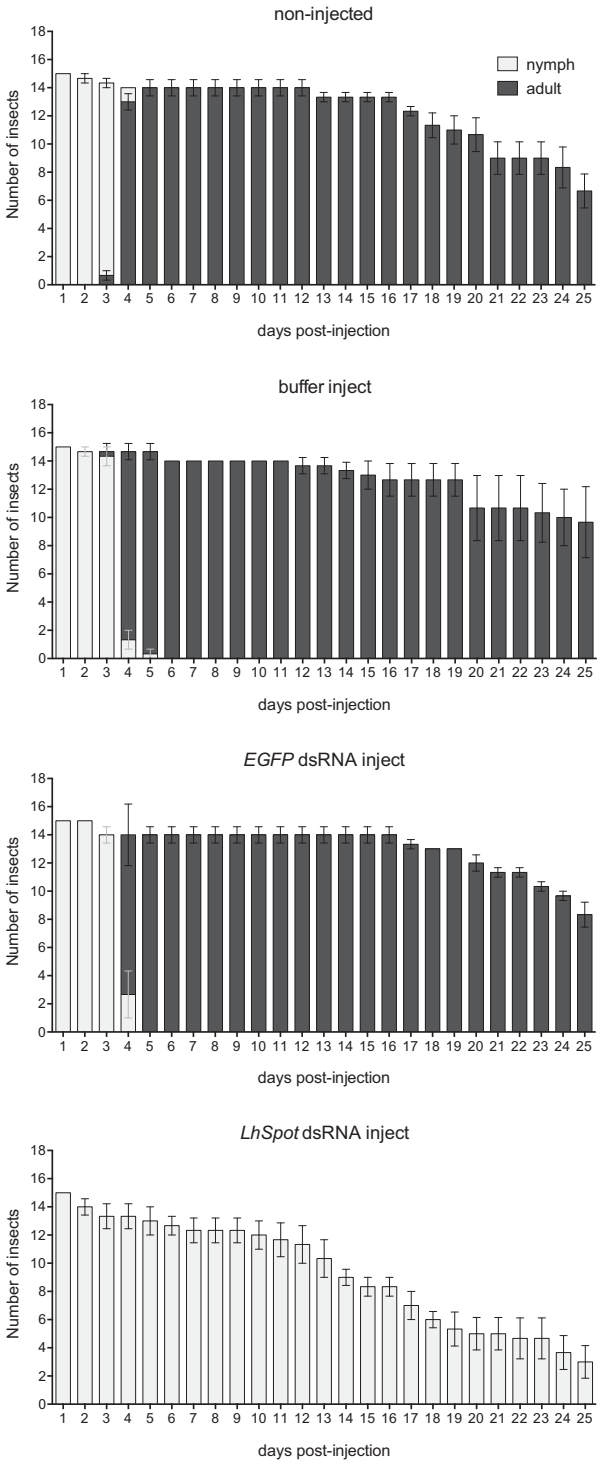

Figure 7. *Lygus hesperus Spookiest (LhSpot)* double-stranded RNA-injected fifth instars do not undergo normal adult development. The developmental status of newly emerged fifth instars was tracked for 25 days after treatment. Data represent mean ± SEM of samples ran in triplicate with 15 insects per treatment. Abbreviation: EGFP, *enhanced green fluorescent protein*.

We next assessed the effects of topically applied 7-dehydrocholesterol, a substrate upstream of the ecdysteroid biosynthesis 'black box'. Unlike 20E, exogenous 7-dehydrocholesterol failed to restore adult eclosion (Fig. 9A), suggesting that LhSpot catalyses an enzymatic step downstream of 7-dehydrocholesterol.

Discussion

Despite extensive molecular and biochemical characterization of the ecdysteroid biosynthetic pathway in holometabolous insects, our understanding of this pathway in hemimetabolous pests, in particular mirids, is extremely limited. To address this deficiency, we sought to mine recent *Ly. hesperus* transcriptome assemblies for potential orthologues of the CYP307 family (Spo, Spok and Spot) of P450 monooxygenases, the proposed rate-limiting enzymes in the 20E biosynthetic pathway. The lone orthologue identified from the search aligned more closely with Spot orthologues than with Spo or Spok orthologues. Consistent with other Spo-like sequences, LhSpot has a membrane-targeting hydrophobic amino terminus followed by a cluster of Arg/Lys residues and a Pro/Gly-rich region that function as a halt-transfer signal and a molecular hinge, respectively, and motifs (the heme-binding loop, helices C, I and K, and PERF domain) characteristic of cytochrome P450s (Werck-Reichhart & Feyereisen, 2000). Close inspection of insect CYP307 sequences reveals a clear differentiation in the region identified as helix C between Spo/Spok and Spot proteins. In Spo/Spok, this region is composed of His/Tyr-Cys-Ser/Gly-Pro, whereas Spot proteins have substituted Thr/Ile-Phe/Glu for the Cys-Ser/Gly pair (Fig. 2). Additional sequence divergence is seen ~20 amino acids upstream of this region in which the conserved Leu in the Ala-Leu-Cys-Asp motif in Spo/Spok proteins is substituted with Phe in Spot proteins. Similar paralogue variation is seen on either side of helix I. On the amino terminal side, the conserved Phe in the Leu-Glu-Asp-Phe sequence in Spo/Spok is substituted with Ile in Spot. On the carboxyl side of helix I, Spot proteins have substituted a charged basic amino acid (Lys) for the hydrophobic residue (Met/Leu) in Spo/Spok (Fig. 2). Although the impact of these amino acid substitutions on the enzymatic activity or substrate specificity of the CYP307 monooxygenases is unknown, we suggest that identification of these sites may facilitate future discrimination and annotation of Spot paralogues in other species.

LhSpot is expressed throughout *Ly. hesperus* development, with transcripts amplified from eggs, all nymphal stages and reproductively mature adults (Fig. 5A). The lone CYP307 paralogue in *Ap. mellifera*, *Spot*, is likewise expressed in multiple life stages (pupa, prepupa and

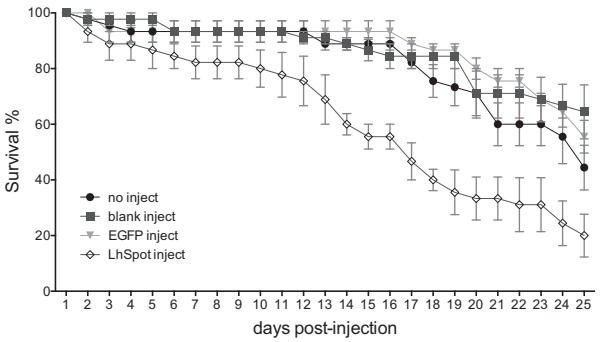

Figure 8. *Lygus hesperus Spookiest (LhSpot)* double-stranded RNA-injected fifth instar females exhibit reduced survivorship. The survivorship of newly emerged fifth instars was tracked for 25 days after treatment. Data represent mean ± SEM of samples ran in triplicate with 15 insects per treatment replicate. Abbreviation: EGFP, *enhanced green fluorescent protein*.

queen ovary; Yamazaki *et al*., 2011). This contrasts with the expression profile reported for the *Spot* orthologue in *T. castaneum*, which was spatially and temporally restricted to the adult male tubular accessory glands (Hentze *et al*., 2013). No amplimer was detected in *Ly. hesperus* accessory glands in our RT-PCR based analyses. This difference may be attributable to very low transcript levels in the accessory glands, which would raise questions regarding functional relevance, or could indicate a temporal aspect to *LhSpot* expression in this tissue. Alternatively, because two CYP307 paralogues (*Spo* and *Spot*) were reported in *T. castaneum*, with *Spo* expression limited to pre-adult stages, it is possible that the two gene products fulfil specific functions that have diverged temporally and spatially. Expression of two paralogues in *Dr. melanogaster* is likewise defined in terms of tissue and developmental stage. The *Dr. melanogaster Spo* is expressed during early embryonic development and adult ovarian maturation, whereas activity of *Spok* is restricted to the prothoracic gland in late embryos and larval stages (Ono *et al*., 2006). Rewitz *et al*. (2007) speculated that the distinct spatial and temporal expression profiles exhibited by the *Spo* paralogues reflect integration of a retrosequence near the promoter region, a genomic event that could alter the tissue expression specificity. Gene duplication resulting in multiple *Spo* paralogues may also have facilitated the development of distinct roles in ecdysteroid development as evidenced by the restricted expression of *Spot* in *T. castaneum*. The tissue-specific expression profile exhibited when multiple *Spo* paralogues are present could be an indication that *LhSpot*, which appears to lack temporal and spatial restrictions on expression, is the lone *Spo* paralogue in *Ly. hesperus*.

For *Ly. hesperus*, circulating ecdysteroids peak ∼48 h after the final nymphal–nymphal moult, with adult eclosion occurring 48 h later (Brent *et al*., 2016). The elevated expression of *LhSpot* at 24 h and subsequent decline (Fig. 5A) correlate well with the biosynthesis of ecdysteroids needed to trigger adult eclosion. *LhSpot* transcript expression, however, exhibits rhythmicity within the fifth-instar stage as evidenced by the expression peaks at 24 and 72 h post-emergence. Similar fluctuations in the expression of Halloween genes have been reported in *La. striatellus* (Jia *et al*., 2013a, 2014, 2015; Wan *et al*., 2014a,b), *Spodoptera littoralis* (Iga & Smagghe, 2010), *Ch. suppressalis* (Shahzad *et al*., 2015), *Bo. mori* (Ono *et al*., 2006), *Manduca sexta* (Ono *et al*., 2006) and *T. castaneum* (Hentze *et al*., 2013). We speculate that the second burst of *LhSpot* expression might be linked with ecdysteroid influence on the pacing of gonadal development, which may be a response to the loss of negative feedback associated with disintegration of the nymphal prothoracic gland (Marchal *et al*., 2010), or may signify a non-ecdysteroidal function of LhSpot. To examine the validity of these possible explanations, however, further studies are needed to develop a more thorough understanding of the physiological and endocrinological mechanisms underlying this process in *Ly. hesperus*.

RNAi-mediated knockdown of *LhSpot* transcripts in newly eclosed fifth instars was apparent within 24 h of dsRNA injection with phenotypic effects that extended throughout normal adult eclosion, which occurred 3–4 days post-injection in control nymphs (Fig. 7). Surprisingly, the *LhSpot* knockdown group never developed external adult features; rather they retained the nymphal form until death, which in some cases was 37 days after fifth instar emergence. Delayed development was reported following RNAi knockdown of *Spo* in *T. castaneum*, which had a 40% moult rate 9 days post-dsRNA treatment (Hentze *et al*., 2013), in *So. furcifera* with 24% remaining as third instars (Jia *et al*., 2013b) and *Ch. suppressalis* with ∼25% remaining as fourth instars (Shahzad *et al*., 2015). Similarly, RNAi knockdown of the larval *Spok* paralogue in *Drosophila* resulted in ∼98% of the larvae remaining as first instars (Ono *et al*., 2006). By contrast, *Spo* knockdown in *Schistocerca gregaria* and *An. gambiae* had no clear developmental phenotype despite reduced ecdysteroid production (Marchal *et al*., 2011; Pondeville *et al*., 2013). The incomplete development that we observed compared with the delayed development reported in other studies could be attributable to methodological variations in dsRNA delivery or biological compensatory effects. For both possibilities, residual enzyme activities resulting from partial or transient knockdown may be sufficient to sustain ecdysteroids at levels necessary to allow continued development. Indeed, *Sc. gregaria Spo* transcript levels in male nymphs rebounded 2 days post-injection

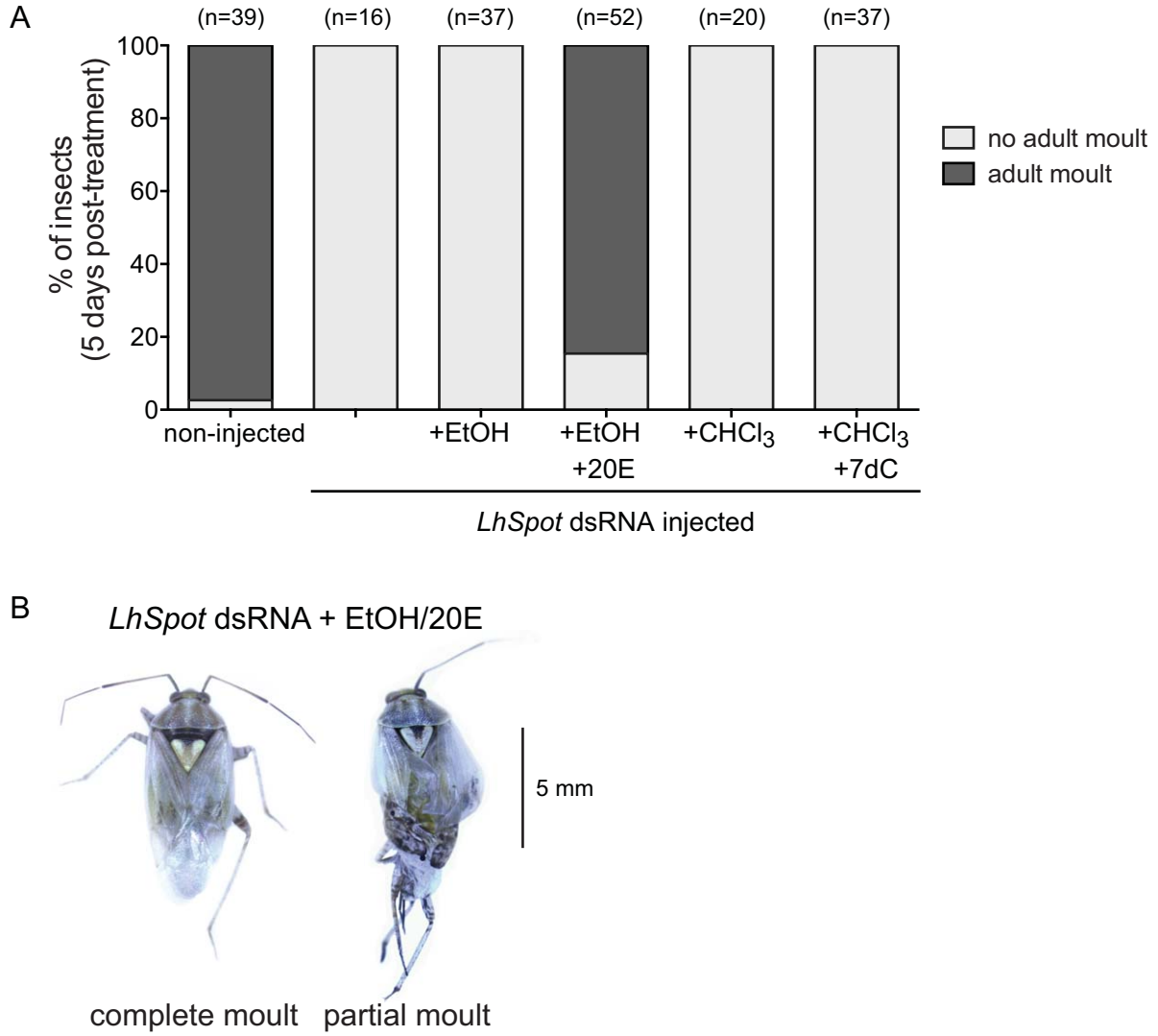

Figure 9. *Lygus hesperus Spookiest (LhSpot)* knockdown effect on adult eclosion is rescued with exogenous 20-hydroxyecdysone (20E). (A) Newly emerged fifth instars injected with *LhSpot* double-stranded RNA (dsRNA) were treated 24 h after injection with handling stimulus alone or topical applications of 90% ethanol (+EtOH), 20E in 90% ethanol (+20E), 100% chloroform (+$CHCl_3$) and 7-dehydrocholesterol in 100% chloroform (+7dC). The developmental status was then tracked over a 5-day period and compared with non-injected nymphs. Under normal conditions, fifth instars typically undergo adult eclosion after 4–5 days at 27°C. The number of surviving individuals assessed at day 5 is indicated above the bars. (B) *LhSpot* knockdown nymphs enter eclosion following exogenous 20E application. Timing of the 20E application is critical to the adult moult as variations in application resulted in nymphs that only underwent a partial moult (right insect).

(Marchal *et al*., 2011). As ecdysteroidogenesis can be regulated by multiple factors (Marchal *et al*., 2010), it is possible that some regulatory feedback mechanism may compensate for the transcript knockdown triggered by the dsRNAs.

The rescue effect associated with exogenous application of an ecdysteroid (eg 20E) upstream of impaired Halloween gene activity has been demonstrated in diverse species including *So. furcifera*, *Dr. melanogaster* and *Ch. suppressalis* (Ono *et al*., 2006; Jia *et al*., 2013a,b; Shahzad *et al*., 2015). Similarly, we found that topical application of 20E at 24 h post-dsRNA injection was sufficient to restore development to adulthood. However, no rescue effect was seen when 20E was applied later than 24 h after injection, suggesting that proper timing of the ecdysone pulse, perhaps in relation to juvenile hormone titres, is critical for normal development to adulthood in *Ly. hesperus*. Consequently, it is possible the addition of exogenous 20E later than 24 h post-injection disrupts the timing, duration and/or interaction framework of the ecdysteroid pulse critical to perpetuate development to completion. Although our understanding of the role that ecdysteroids have in hemimetabolous insects continues to develop, it is clear that 20E affects

an intricate transcriptional regulation cascade, disruption of which can lead to uncoordinated development, poorly timed moults and impaired ecdysis (Cruz *et al*., 2008; Mané-Padrós *et al*., 2010, 2012).

In some female insects, ovarian-based ecdysteroidogenesis is required for oogenesis (Terashima *et al*., 2005; Parthasarathy *et al*., 2010), with Halloween gene expression reported in female reproductive tissues of *Dr. melanogaster* (Ono *et al*., 2006), *Sc. gregaria* (Marchal *et al*., 2011), *Holcocerus hippophaecolus* (Zhou *et al*., 2013), *An. gambiae* (Pondeville *et al*., 2013) and *T. castaneum* (Parthasarathy *et al*., 2010). RNAi-mediated knockdown of *Spo* and *Phantom* in *An. gambiae* and *T. castaneum*, respectively, impeded ovarian ecdysteroid production (Pondeville *et al*., 2013), whereas in *T. castaneum* knockdown of *Shade*, the terminal enzyme in the ecdysteroid biosynthetic pathway, severely impaired ovarian growth and primary oocyte maturation (Parthasarathy *et al*., 2010). Similarly, *Dr. melanogaster* females with a mutation in *Spo* failed to produce progeny when mated with fertile wild-type males and had arrested egg development (Ono *et al*., 2006). The expression of *LhSpot* in adult female reproductive tissues (Fig. 5B) is consistent with the role described above for Halloween genes in ovarian maturation. Given the necessity of ecdysteroid production for egg development, it was surprising to observe oogenesis comparable to a reproductive 3-day-old adult female in *LhSpot* dsRNA-injected nymphs that had failed to undergo adult eclosion (Fig. 6C). The external characteristics of these nymphs were phenotypically fifth instar in appearance without wings or a protruding ovipositor. We speculate that the internal development of adult characteristics (ie oogenesis) is dependent on ecdysteroid biosynthesis and was able to proceed because the knockdown effects had diminished. Alternatively, because RNAi-induced knockdown does not completely eliminate the target protein, residual enzyme activities may be sufficient to sustain a level of 20E synthesis above the threshold needed for oogenesis. These findings also suggest that the transcriptional timing of the two ecdysteroid-linked events, adult eclosion and oogenesis, is disconnected. The exact role of *LhSpot* in oogenesis and the degree of linkage between the ecdysteroid events remain to be fully explored.

This is, to our knowledge, the first *in vivo* demonstration of Spot function in insect development. Here, we have shown that the LhSpot sequence aligns phylogenetically with CYP307B1 proteins, that it is expressed throughout *Ly. hesperus* development, and is expressed in female reproductive tissues. The phenotypic effects observed in immatures (uncoordinated development, arrested adult eclosion) following RNAi knockdown, expression throughout larval and adult development, and singularity in our transcriptome assembly, suggest that, as in *Ap. mellifera*, the *LhSpot* paralogue is the only CYP307 gene in *Ly. hesperus*. The presence of multiple *Spo*/*Spok*/*Spot* paralogues in the genomes of two hemipteran pests, *Ac. pisum* and *Ni. lugens*, suggests that loss of a former gene duplication may be a relatively recent evolutionary event.

Experimental procedures

Insects

Lygus hesperus were reared in a laboratory colony at the United States Department of Agriculture (USDA) Agricultural Research Service, Arid Land Agricultural Research Center (Maricopa, AZ, USA) and maintained on a mix of green bean pods (*Phaseolus vulgaris* L.) and an *ad libitum* artificial diet mix (Debolt, 1982) packaged in Parafilm M (Pechiney Plastic Packaging, Chicago, IL, USA) as described previously (Patana, 1982). Insects were reared under a light : dark 14:10 h photoperiod at $27 \pm 1\,^{\circ}C$ and 40–60% relative humidity (RH). Eggs were deposited in oviposition packets (Parafilm M filled with agarose gel). Daily monitoring of experimental insects ensured timely collection of individuals within 24 h of nymphal moult or adult eclosion.

Transcriptomic identification and bioinformatic characterization of a Lygus *Spo-like sequence*

To identify putative *Ly. hesperus Spo* paralogues, we used the tBLASTn program to search (*e*-value $\leq 10^{-5}$) our previously assembled *Ly. hesperus* transcriptome (Hull *et al*., 2014) using queries consisting of Spo sequences from six insect species: *Dr. melanogaster* (NP_647975), *Bo. mori* (NP_001104833), *Na. vitripennis* (XP_001603435), *T. castaneum* (XP_974280), *Ac. pisum* (XP_001945761) and *La. striatellus* (AFU86444). The longest isoform from the resulting *Ly. hesperus* sequence hit was then re-evaluated by BLASTx (*e* value $\leq 10^{-5}$) using the National Center for Biotechnology Information (NCBI) non-redundant (nr) database.

To determine phylogenetic relationships, a MUSCLE-based multiple sequence alignment (Edgar, 2004) consisting of the putative *Ly. hesperus* Spo-like (LhSpot) sequence and protein sequences for the suite of Halloween genes from five species (Table S1) was performed using default settings in Geneious 7.1.8 (Biomatters Ltd., Auckland, New Zealand). Phylogenetic trees were constructed using the maximum likelihood, minimum evolution, UPGMA and neighbour-joining methods in MEGA6 v. 6.06 r6140220 (Tamura *et al*., 2013). A more detailed analysis of the potential phylogenetic relationships between the putative LhSpot and the sequences that comprise the CYP307A1/CYP307A2/CYP307B1 (ie Spo/Spok/Spot) group of enzymes was performed using 20 sequences annotated accordingly in the NCBI database. The evolutionary history was inferred as before in MEGA6 using the maximum likelihood method. Initial tree(s) for the heuristic search were obtained by applying the neighbour-joining method to a matrix of pairwise distances estimated using a Jones Thornton-Taylor (JTT) model. The tree was drawn to scale, with branch lengths measured in the number of substitutions per site. The analysis involved 21 amino acid sequences, with all positions containing gaps and missing data eliminated, resulting in a final data set consisting of 58 total positions. WoLF PSORT (Horton *et al*.,

2007) and the Target P 1.1 server (Emanuelsson *et al.*, 2007) were used for subcellular localization prediction.

Cloning and transcriptional profiling of LhSpot

To generate a full-length clone of *LhSpot*, total RNA was isolated from five mixed gender fifth-instar nymphs pooled at 2 days post-eclosion (period when circulating ecdysteroid levels are highest; Brent *et al.*, 2016) using TRI Reagent (Life Technologies, Carlsbad, CA, USA) as described by Chomczynski & Sacchi (1987). First-strand cDNAs were generated using Superscript III reverse transcriptase (Life Technologies) with custom-made random pentadecamers (IDT, San Diego, CA, USA) and 500 ng DNase I-treated total RNAs. Full-length *LhSpot* was amplified using primers (Table S2) designed to span the predicted ORF of the putative *LhSpot* identified in our transcriptome database search. Multiple independent reactions were performed using Premix ExTaq (Clontech Laboratories, Mountain View, CA, USA) in a 20-μl volume with 1 μl cDNA template (25 ng) and 0.2 μM of each primer. Thermocycler conditions consisted of 95 °C for 2 min followed by 35 cycles at 94 °C for 20 s, 55 °C for 20 s, 72 °C for 90 s, and a final extension at 72 °C for 5 min. Amplimers were separated on 1.5% agarose gels using a Tris/acetate/ethylenediaminetetraacetic acid buffer system and visualized with SYBR Safe (Life Technologies). Products from each reaction were subcloned using a pCR2.1-TOPO TA cloning kit (Life Technologies) and sequenced at the Arizona State University DNA Core Laboratory (Tempe, AZ, USA).

To examine the expression profile of *LhSpot*, total RNAs were isolated as above from pooled samples of eggs, each of the first four nymphal instars, as well as fifth instars at 0, 1, 2 and 3 days post-ecdysis, and mixed gender adults sampled at 0, 1 and 2 days post-eclosion. For first and second instars, 20 mixed-gender nymphs were used. For third-fifth instars, 10 mixed-gender nymphs were pooled. For adult samples, five of each gender were pooled. Parallel analyses examining the tissue distribution of the *LhSpot* transcript used total RNAs isolated from mixed-gender fifth instars and adults of each gender: 15 heads, five thoraces and five abdomens for fifth instars, 25 mixed hindgut/midgut for adults, five pairs of pooled lateral and medial accessory glands, five pairs of testes and pooled samples of five pairs of ovaries and 20 seminal depositories. Expression profiles for each sample were generated using Sapphire Amp Fast PCR Master Mix (Clontech Laboratories), 12.5 ng of each respective cDNA template, and 0.2 μM of primers (Table S2) designed to amplify nt 1–555 of a reference gene, *Lygus actin* (DQ386914), or a fragment of *LhSpot* (nt 1–498). Thermocycler conditions consisted of 95 °C for 2 min followed by 35 cycles at 94 °C for 20 s, 56 °C for 20 s and 72 °C for 30 s, and a final extension at 72 °C for 5 min. PCR products were separated on 1.5% agarose gels as before with representative amplimers subcloned into pCR2.1-TOPO and the sequences verified.

Transient expression of a fluorescent LhSpot chimera in cultured insect cells

To examine the intracellular localization of LhSpot, insect expression vectors encoding fluorescent chimeras of LhSpot and an endoplasmic reticulum marker (KDEL receptor 1) were constructed. Overlap extension PCR (Wurch *et al.*, 1998) using KOD Hot Start DNA polymerase (Toyobo/Novagen, EMD Biosciences, San Diego, CA, USA) was used to generate the respective chimeras with mVenus or mCherry fused in-frame to the carboxyl terminal residues of LhSpot (LhSpot-Venus) and the *Homo sapiens* KDEL endoplasmic reticulum protein retention receptor 1 (HsKDELR-mCherry), respectively. The initial PCR products were generated from plasmid DNA templates (pCR2.1TOPO/LhSpot, above; pOTB7/HsKDELR, NM_006801.2; Transomic Technologies, Huntsville, AL, USA; and pIB vectors containing either mVenus or mCherry) using gene-specific and chimeric primers (Table S2). Thermocycler conditions consisted of 95 °C for 2 min followed by 21 cycles at 95 °C for 20 s, 58 °C for 20 s and 70 °C for 60 s, with a final incubation at 70 °C for 5 min. Amplimers of the expected sizes were gel excised and purified using an EZNA Gel Extraction kit (Omega Bio-Tek Inc., Norcross, GA, USA). The respective 5' and 3' fragments were joined using KOD Hot Start DNA polymerase with gene-specific primers (Table S2). Thermocycler conditions consisted of 95 °C for 2 min followed by 25 cycles at 95 °C for 20 s, 56 °C for 20 s, and 70 °C for 90 s with a final incubation at 70 °C for 5 min. The resulting PCR products were gel excised, treated with ExTaq DNA polymerase (Clontech) to add 3'A overhangs, cloned into the pIB/V5-His TOPO TA insect expression vector (Life Technologies) and the sequences verified.

Trichoplusia ni cells (Orbigen Inc., San Diego, CA, USA), maintained as adherent cultures in serum-free insect culture media (Orbigen Inc.), were seeded into 35-mm #1.5 glass bottom dishes (MatTek Corp., Ashland, MA, USA) and allowed to settle for 20 min. Cells were then co-transfected with 2 μg of each plasmid (pIB/LhSpot-Venus and pIB/HsKDELR-mCherry) using 8 μl Insect Gene Juice transfection reagent (Novagen, EMD Biosciences, San Diego, CA, USA) for 5 h. Transfection media was then removed, the cells washed twice with 1 ml serum-free media and then maintained in serum-free media at 28 °C. After 48 h, the transfected cells were washed twice with 1 ml IPL-41 insect media (Life Technologies) and then imaged in 2 ml IPL-41 using a 60× phase contrast water-immersion objective (numerical aperture 1.2) on a Fluoview FV10i-LIV laser scanning confocal microscope (Olympus, Center Valley, PA, USA). Images were subsequently processed (tone and contrast) in Adobe Photoshop CS6 (Adobe System Inc., San Jose, CA, USA).

dsRNA synthesis and injection

dsRNA was produced using a MEGAscript RNAi kit (Life Technologies) according to the manufacturer's instructions. A 547-bp fragment corresponding to nt 846–1352 of the *LhSpot* ORF was amplified from plasmid DNA using Sapphire Amp Fast PCR Master Mix with primers containing a 5' T7 promoter sequence (Table S2). The amplified fragment was TOPO-cloned into pCR2.1-TOPO (Life Technologies) and chemically competent TOP10 *Escherichia coli* cells (Life Technologies) were transformed. As a negative control, a dsRNA targeting the complete ORF of *EGFP* was generated using similar primers (Table S2). The template in the T7 reaction was amplified from the plasmid DNA with Sapphire Amp Fast PCR Master Mix and gel purified using the EZNA gel extraction kit. After transcription, the

dsRNAs were digested with nuclease to remove residual template DNA and non-annealed single-stranded RNA and then purified according to the manufacturer's instructions on columns provided with the MEGAscript RNAi kit. The dsRNA fragments were quantitated using the Take3 multi-volume plate on a Synergy H4 hybrid multi-mode microplate reader (BioTek Instruments, Winooski, VT, USA) and then diluted to a concentration of 1 μg/μl in MEGAscript RNAi kit elution buffer (EB).

Injection needles were made from 5-μl disposable soda lime glass pipettes (Thermo Fisher, Kimble Chase, Pittsburgh, PA, USA) using a Narishige PN-30 Magnetic Glass Microelectrode Horizontal Puller (Narishige International, Amityville, NY, USA) at heater level 84.4 and magnet level 25.5. To facilitate injection, sharp edges were made by snapping off the needle tips. The manual dsRNA delivery system consisted of a 60-cm-long tygon tube with a 1000-μl pipette tip inserted into one end (narrow tip protruding for clasping the pulled glass needles) and a second 1000-μl pipette tip inserted in the opposite orientation at the other end of the tube. The glass needles were fastened in the narrow opening with Parafilm M. To calibrate the needles, 0.25 μl (for nymphs) or 0.5 μl (for adults) of RNase-free water pipetted with a 2.5-μl pipettor was drawn directly from the pipette tip using the manual injection system. The needles were marked and the calibration was repeated three times to ensure accuracy. Before injection, the insects were immobilized by cooling at 4 °C for 20 min. A freezer icepack, cleaned with ethanol, was used as the injection stage. Insects were injected on the ventral right side between the fifth and seventh abdominal tergites, then allowed to recover for 10 min. Those failing to recuperate were discarded. Survivors were maintained at 27 °C and 30% RH in Huhtamaki waxed cups (Huhtamaki, De Soto, KS, USA) with a mesh screen, and provided green bean pods (*Ph. vulgaris* L.) every 2 days.

Fifth instars were collected within 24 h of the nymphal moult. Three biological replicates were conducted, each having four treatment groups: non-injected controls; nymphs injected with 0.25 μl EB; nymphs injected with 250 ng/0.25 μl *EGFP* dsRNA; and nymphs injected with 250 ng/0.25 μl *LhSpot* dsRNA. Each treatment and replicate consisted of 15 nymphs, which were monitored daily for the incidence and timing of adult eclosion. After a minimum of 25 days post-injection, survivors were dissected and phenotype images collected using a Leica DFC425 camera attached to a Leica M165C microscope with an LED ring light (Leica Microsystems, Buffalo Grove, IL, USA).

RT-PCR verification of RNAi-mediated LhSpot *knockdown*

Total RNA was isolated from fifth instars (three per treatment) as described above. Potentially contaminating genomic DNA was removed using a DNA-free DNA removal kit (Life Technologies) according to the manufacturer's instructions. First-strand cDNA was synthesized from 2 μg DNase-free RNA with a RETROscript kit (Life Technologies) in a 20-μl reaction according to the manufacturer's instructions using the supplied oligo-(dT) primer. Full-length *Ly. hesperus GAPDH* (nt 1–1002; Transcriptome Shotgun Assembly (TSA) accession GBHO01012854) and ~500-bp fragments of *Lygus actin* (nt 1–555), the ecdysone responsive genes *E74* (nt 61–568; TSA accession GBHO01008524) and *E75* (nt 1–556; TSA accession GBHO01011368), and *LhSpot* (nt 1–498) were PCR amplified using Sapphire Amp Fast PCR Master Mix in a 20-μl reaction containing 0.5 μl cDNA template (50 ng) and 0.2 μM of each primer (Table S2). Thermocycler conditions consisted of initial denaturation at 95 °C for 2 min followed by 35 cycles at 95 °C for 20 s, 56 °C for 20 s, and 72 °C for 60 s with a final extension at 72 °C for 5 min. PCR products were electrophoresed as before but using 1% agarose gels containing SYBR Safe. Amplimers were visualized using an ImageReader LAS4000 (Fujifilm, Tokyo, Japan), subcloned as before and the sequences validated.

Exogenous application of 20E and 7-dehydrocholesterol

In total, 280 fifth-instar females over three experimental replicates were collected within 24 h of moulting and injected with 250 ng/0.25 μl *LhSpot* dsRNA. Injected nymphs were placed in groups of 10 within Petri dishes (10 × 1.5 cm) for overnight maintenance. At 24 h post-injection, the insects were collected together in a single vial and dead nymphs removed. The insects were immobilized by cooling at 4 °C for 20 min and then treated with 0.25 μl (1 μg/μl) 20E (Sigma-Aldrich, St Louis, MO, USA) in 90% ethanol, 0.25 μl 90% ethanol alone, 0.25 μl (1 μg/μl) 7-dehydrocholesterol (Sigma-Aldrich) in 100% chloroform, or 0.25 μl 100% chloroform alone. One Petri dish was used for every 10 treated nymphs and the nymphs were allowed to recover for 2 h, after which dead nymphs were removed. A non-replicated group of 30 non-injected female nymphs, subject only to handling stress, was also monitored for adult eclosion under the same conditions (10 insects/Petri dish). Petri dishes with insects were maintained at 27 °C and 30% RH and provided with a green bean pod section that was replaced every 2 days. Insects were surveyed daily to determine timing of the adult moult.

Acknowledgements

The authors thank Daniel Langhorst for maintaining the *Ly. hesperus* colony and Lynn Forlow Jech for assistance with tissue dissections and insect cell culture maintenance. Funding was provided by the China Scholarship Council to M.W. and by Cotton Inc. (12-373) to C.S.B. and J.J.H. Mention of trade names or commercial products in this article is solely for the purpose of providing specific information and does not imply recommendation or endorsement by the U. S. Department of Agriculture. USDA is an equal opportunity provider and employer.

References

Brent, C.S., Wang, M., Miao, Y.-G. and Hull, J.J. (2016) Ecdysteroid and chitinase fluctuations in the western tarnished plant bug (*Lygus hesperus*) prior to molt indicate roles in development. *Arch Insect Biochem Physiol* **92**: 108–126.

Cabrera, A.R., Shirk, P.D., Evans, J.D., Hung, K., Sims, J., Alborn, H. *et al.* (2015) Three Halloween genes from the

Varroa mite, *Varroa destructor* (Anderson & Trueman) and their expression during reproduction. *Insect Mol Biol* **24**: 277–292.

Canavoso, L.E., Jouni, Z.E. and Karnas, K.J. (2001) Fat metabolism in insects. *Ann Rev Nutr* **21**: 23–46.

Chomczynski, P. and Sacchi, N. (1987) Single-step method of RNA isolation by acid guanidinium thiocyanate-phenol-chloroform extraction. *Anal Biochem* **162**: 156–159.

Christiaens, O., Iga, M., Velarde, R.A., Rougé, P. and Smagghe, G. (2010) Halloween genes and nuclear receptors in ecdysteroid biosynthesis and signalling in the pea aphid. *Insect Mol Biol* **19**: 187–200.

Cruz, J., Nieva, C., Mané-Padrós, D., Martín, D. and Bellés, X. (2008) Nuclear receptor BgFTZ-F1 regulates molting and the timing of ecdysteroid production during nymphal development in the hemimetabolous insect *Blattella germanica*. *Dev Dyn* **237**: 3179–3191.

Dai, L., Ma, M., Wang, C., Shi, Q., Zhang, R. and Chen, H. (2015) Cytochrome P450s from the Chinese white pine beetle, *Dendroctonus armandi* (Curculionidae: Scolytinae): expression profiles of different stages and responses to host allelochemicals. *Insect Biochem Mol Biol* **65**: 35–46.

Debolt, J.W. (1982) Meridic diet for rearing successive generations of *Lygus hesperus*. *Ann Entomol Soc Am* **75**: 119–122.

Edgar, R.C. (2004) MUSCLE: multiple sequence alignment with high accuracy and high throughput. *Nucleic Acids Res* **32**: 1792–1797.

Emanuelsson, O., Brunak, S., von Heijne, G. and Nielsen, H. (2007) Locating proteins in the cell using TargetP, SignalP and related tools. *Nat Protoc* **2**: 953–971.

Gilbert, L.I. and Warren, J.T. (2005) A molecular genetic approach to the biosynthesis of the insect steroid molting hormone. *Vitam Horm* **73**: 31–57.

Gilbert, L.I., Rybczynski, R. and Warren, J.T. (2002) Control and biochemical nature of the ecdysteroidogenic pathway. *Annu Rev Entomol* **47**: 883–916.

Hentze, J.L., Moeller, M.E., Jørgensen, A.F., Bengtsson, M.S., Bordoy, A.M., Warren, J.T. *et al*. (2013) Accessory gland as a site for prothoracicotropic hormone controlled ecdysone synthesis in adult male insects. *PLoS ONE* **8**: e55131.

Horton, P., Park, K.J., Obayashi, T., Fujita, N., Harada, H., Adams-Collier, C.J. and Nakai, K. (2007) WoLF PSORT: protein localization predictor. *Nucleic Acids Res* **35**: W585–W587.

Hull, J.J., Geib, S.M., Fabrick, J.A. and Brent, C.S. (2013) Sequencing and de novo assembly of the western tarnished plant bug (*Lygus hesperus*) transcriptome. *PLoS ONE* **8**: e55105.

Hull, J.J., Chaney, K., Geib, S.M., Fabrick, J.A., Brent, C.S., Walsh, D. and Lavine, L.C. (2014) Transcriptome-based identification of ABC transporters in the western tarnished plant bug *Lygus hesperus*. *PLoS ONE* **9**: e113046.

Iga, M. and Kataoka, H. (2012) Recent studies on insect hormone metabolic pathways mediated by cytochrome P450 enzymes. *Biol Pharm Bull* **35**: 838–843.

Iga, M. and Smagghe, G. (2010) Identification and expression profile of Halloween genes involved in ecdysteroid biosynthesis in *Spodoptera littoralis*. *Peptides* **31**: 456–467.

Jia, S., Wan, P.J., Zhou, L.T., Mu, L.L. and Li, G.Q. (2013a) Knockdown of a putative Halloween gene Shade reveals its role in ecdysteroidogenesis in the small brown planthopper *Laodelphax striatellus*. *Gene* **531**: 168–174.

Jia, S., Wan, P.J., Zhou, L.T., Mu, L.L. and Li, G.Q. (2013b) Molecular cloning and RNA interference-mediated functional characterization of a Halloween gene spook in the white-backed planthopper *Sogatella furcifera*. *BMC Mol Biol* **14**: 19–28.

Jia, S., Wan, P.J. and Li, G.Q. (2014) Molecular cloning and characterization of the putative Halloween gene Phantom from the small brown planthopper *Laodelphax striatellus*. *Insect Sci* **00**: 1–12.

Jia, S., Wan, P.J., Zhou, L.T., Mu, L.L. and Li, G.Q. (2015) RNA interference-mediated silencing of a Halloween gene spookier affects nymph performance in the small brown planthopper *Laodelphax striatellus*. *Insect Sci* **22**: 191–202.

Jürgens, G., Wieschaus, E., Nüsslein-Volhard, C. and Kluding, H. (1984) Mutations affecting the pattern of the larval cuticle in *Drosophila melanogaster*. II. Zygotic loci on the third chromosome. *Roux's Arch Dev Biol* **193**: 283–295.

Koolman, J. (1982) Ecdysone metabolism. *Insect Biochem* **12**: 225–250.

Luan, J.B., Ghanim, M., Liu, S.S. and Czosnek, H. (2013) Silencing the ecdysone synthesis and signaling pathway genes disrupts nymphal development in the whitefly. *Insect Biochem Mol Biol* **43**: 740–746.

Mané-Padrós, D., Cruz, J., Vilaplana, L., Nieva, C., Ureña, E., Bellés, X. *et al*. (2010) The hormonal pathway controlling cell death during metamorphosis in a hemimetabolous insect. *Dev Biol* **346**: 150–160.

Mané-Padrós, D., Borràs-Castells, F., Bellés, X. and Martín, D. (2012) Nuclear receptor HR4 plays an essential role in the ecdysteroid-triggered gene cascade in the development of the hemimetabolous insect *Blattella germanica*. *Mol Cell Endocrinol* **348**: 322–330.

Marchal, E., Vandersmissen, H.P., Badisco, L., Van de Velde, S., Verlinden, H., Iga, M. *et al*. (2010) Control of ecdysteroidogenesis in prothoracic glands of insects: a review. *Peptides* **31**: 506–519.

Marchal, E., Badisco, L., Verlinden, H., Vandersmissen, T., Van Soest, S., Van Wielendaele, P. *et al*. (2011) Role of the Halloween genes, Spook and Phantom in ecdysteroidogenesis in the desert locust, *Schistocerca gregaria*. *J Insect Physiol* **57**: 1240–1248.

Maroniche, G.A., Mongelli, V.C., Alfonso, V., Llauger, G., Taboga, O. and del Vas, M. (2011) Development of a novel set of Gateway-compatible vectors for live imaging in insect cells. *Insect Mol Biol* **20**: 675–685.

Morgan, E.D. and Poole, C.F. (1977) Chemical control of insect moulting. *Comp Biochem Physiol B* **57**: 99–109.

Namiki, T., Niwa, R., Sakudoh, T., Shirai, K.I., Takeuchi, H. and Kataoka, H. (2005) Cytochrome P450 CYP307A1/Spook: a regulator for ecdysone synthesis in insects. *Biochem Biophys Res Commun* **337**: 367–374.

Niwa, R. and Niwa, Y.S. (2011) The fruit fly *Drosophila melanogaster* as a model system to study cholesterol metabolism and homeostasis. *Cholesterol* **2011**: 176802.

Niwa, R. and Niwa, Y.S. (2014) Enzymes for ecdysteroid biosynthesis: their biological functions in insects and beyond. *Biosci Biotechnol Biochem* **78**: 1283–1292.

Nüsslein-Volhard, C., Wieschaus, E. and Kluding, H. (1984) Mutations affecting the pattern of the larval cuticle in *Drosophila melanogaster*. I. Zygotic loci on the second chromosome. *Roux's Arch Dev Biol* **183**: 267–282.

Ono, H., Rewitz, K.F., Shinoda, T., Itoyama, K., Petryk, A., Rybcynski, R. *et al*. (2006) Spook and Spookier code for stage-specific components of the ecdysone biosynthesis pathway in Diptera. *Dev Biol* **298**: 555–570.

Ono, H., Morita, S., Asakura, I. and Nishida, R. (2012) Conversion of 3-oxo steroids into ecdysteroids triggers molting and expression of 20E-inducible genes in *Drosophila melanogaster*. *Biochem Biophys Res Commun* **421**: 561–566.

Parthasarathy, R., Sheng, Z., Sun, Z. and Palli, S.R. (2010) Ecdysteroid regulation of ovarian growth and oocyte maturation in the red flour beetle, *Tribolium castaneum*. *Insect Biochem Mol Bio* **40**: 429–439.

Patana, R. (1982) Disposable diet packet for feeding and oviposition of *Lygus hesperus* (Hemiptera: Miridae). *J Econ Entomol* **75**: 668–669.

Pondeville, E., David, J.P., Guittard, E., Maria, A., Jacques, J.C., Ranson, H. *et al.* (2013) Microarray and RNAi analysis of P450s in *Anopheles gambiae* male and female steroidogenic tissues: CYP307A1 is required for ecdysteroid synthesis. *PLoS ONE* **8**: e79861.

Rewitz, K.F. and Gilbert, L.I. (2008) Daphnia Halloween genes that encode cytochrome P450s mediating the synthesis of the arthropod molting hormone: evolutionary implications. *BMC Evol Biol* **8**: 60.

Rewitz, K.F., O'Connor, M.B. and Gilbert, L.I. (2007) Molecular evolution of the insect Halloween family of cytochrome P450s: phylogeny, gene organization and functional conservation. *Insect Biochem Mol Biol* **37**: 741–753.

Schuh, R.T. (2013) *On-line Systematic Catalog of Plant Bugs (Insecta: Heteroptera: Miridae).* http://research.amnh.org/pbi/catalog/. Accessed on 13 January 2016.

Schwartz, M.D. and Foottit, R.G. (1998) *Revision of the Nearctic species of the genus Lygus Hahn, with a review of the Palaearctic species (Heteroptera: Miridae)*. Mem Entomol Int Vol. 10. Associated Publishers, Gainesville, Fla.

Shahzad, M.F., Li, Y., Ge, C., Sun, Y., Yang, Q. and Li, F. (2015) Knockdown of Cs-Spook induces delayed larval molting in rice striped stem borer *Chilo suppressalis*. *Arch Insect Biochem Physiol* **88**: 179–191.

Snodgrass, G.L. (1996) Insecticide resistance in field populations of the tarnished plant bug (Heteroptera: Miridae) in cotton in the Mississippi Delta. *J Econ Entomol* **89**: 783–790.

Snodgrass, G. and Scott, W. (2002) Tolerance to acephate in tarnished plant bug (Heteroptera: Miridae) populations in the Mississippi river delta. *Southwest Entomol* **27**: 191–199.

Snodgrass, G., Gore, J., Abel, C. and Jackson, R. (2009) Acephate resistance in populations of the tarnished plant bug (Heteroptera: Miridae) from the Mississippi River Delta. *J Econ Entomol* **102**: 699–707.

Spurgeon, D.W. and Brent, C.S. (2010) Morphological characters of diapause in *Lygus hesperus* Knight (Hemiptera: Miridae). *J Entomol Sci* **45**: 303–316.

Sztal, T., Chung, H., Gramzow, L., Daborn, P.J., Batterham, P. and Robin, C. (2007) Two independent duplications forming the *Cyp307a* genes in *Drosophila*. *Insect Biochem Mol Biol* **37**: 1044–1053.

Tamura, K., Stecher, G., Peterson, D., Filipski, A. and Kumar, S. (2013) MEGA6: molecular Evolutionary Genetics Analysis Version 6.0. *Mol Biol Evol* **30**: 2725–2729.

Terashima, J., Takaki, K., Sakurai, S. and Bownes, M. (2005) Nutritional status affects 20-hydroxyecdysone concentration and progression of oogenesis in *Drosophila melanogaster*. *J Endocrinol* **187**: 69–79.

Thummel, C.S. (1996) Flies on steroids - *Drosophila* metamorphosis and the mechanisms of steroid hormone action. *Trends Genet* **12**: 306–310.

Truman, J.W. (2005) Hormonal control of insect ecdysis: endocrine cascades for coordinating behaviour with physiology. *Vitam Horm* **73**: 1–30.

van der Vlies, D., Pap, E.H.W., Post, J.A., Celis, J.E. and Wirtz, K.W.A. (2002) Endoplasmic reticulum resident proteins of normal human dermal fibroblasts are the major targets for oxidative stress induced by hydrogen peroxide. *Biochem J* **366**: 825–830.

Wan, P.J., Jia, S., Li, N., Fan, J.M. and Li, G.Q. (2014a) A Halloween gene *shadow* is a potential target for RNA-interference-based pest management in the small brown planthopper *Laodelphax striatellus*. *Pest Manag Sci* **71**: 199–206.

Wan, P.J., Jia, S., Li, N., Fan, J.M. and Li, G.Q. (2014b) RNA interference depletion of the Halloween gene *disembodied* implies its potential application for management of planthopper *Sogatella furcifera* and *Laodelphax striatellus*. *PLoS ONE* **9**: e86675–e86612.

Wan, P.J., Jia, S., Li, N., Fan, J.M. and Li, G.Q. (2014c) The putative Halloween gene *phantom* involved in ecdysteroidogenesis in the white-backed planthopper *Sogatella furcifera*. *Gene* **548**: 112–118.

Wang, B., Shahzad, M.F., Zhang, Z., Sun, H., Han, P., Li, F. *et al.* (2014) Genome-wide analysis reveals the expansion of Cytochrome P450 genes associated with xenobiotic metabolism in rice striped stem borer, *Chilo suppressalis*. *Biochem Biophys Res Commun* **443**: 756–760.

Werck-Reichhart, D. and Feyereisen, R. (2000) Cytochromes P450: a success story. *Genome Biol* **1**: REVIEWS3003.

Wheeler, A.G. (2001) *Biology of the Plant Bugs (Hemiptera: Miridae): Pests, Predators, Opportunists*. Comstock Publishing Associates, New York.

Wieschaus, E., Nüsslein-Volhard, C. and Jürgens, G. (1984) Mutations affecting the pattern of the larval cuticle in *Drosophila melanogaster*. III Zygotic loci on the X-chromosome and fourth chromosome. *Roux's Arch Dev Biol* **193**: 296–307.

Wurch, T., Lestienne, F. and Pauwels, P. (1998) A modified overlap extension PCR method to create chimeric genes in the absence of restriction enzymes. *Biotechnol Tech* **12**: 653–657.

Yamazaki, Y., Kiuchi, M., Takeuchi, H. and Kubo, T. (2011) Ecdysteroid biosynthesis in workers of the European honeybee *Apis mellifera* L. *Insect Biochem Mol Biol* **41**: 283–293.

Zhou, J., Zhang, H., Li, J., Sheng, X., Zong, S., Luo, Y. *et al.* (2013) Molecular cloning and expression profile of a Halloween gene encoding CYP307A1 from the seabuckthorn carpenterworm, *Holcocerus hippophaecolus*. *J Insect Sci* **13**: 56.

Supporting Information

Additional Supporting Information may be found in the online version of this article at the publisher's web-site:

Table S1. MUSCLE-based multiple sequence alignment heat map of the per cent amino acid identities amongst select insect spook (Spo)/spookier (Spok)/Spookiest (Spot) sequences.

Table S2. List of oligonucleotide primers.

Table S3. Accession/model numbers for Halloween sequences used in phylogenetic analyses.